Research Square

Preprints are preliminary reports that have not undergone peer review.
They should not be considered conclusive, used to inform clinical practice,
or referenced by the media as validated information.

Radio-sensitization of mutated KRAS G12C non-small cell lung cancer with KRAS G12C tyrosine kinase inhibitor and Carbon ions irradiation

Mathieu Césaire
Centre de Recherche sur les Ions, les Matériaux et la Photonique
Kilian Lecrosnier
Centre de Recherche sur les Ions, les Matériaux et la Photonique
Juliette Montanari
Centre de Recherche sur les Ions, les Matériaux et la Photonique
Mateusz Sitarz
Centre de Recherche sur les Ions, les Matériaux et la Photonique
Sahra Messaoudi
Unité de recherche interdisciplinaire pour la prévention et le traitement des cancers
Elisabeth Chartier-Garcia
Laboratoire de Chimie et Biologie des Métaux
Isabelle Testard
Laboratoire de Chimie et Biologie des Métaux
Guénaëlle Levallet
UMR6030 ISTCT
François Christy
Center François Baclesse
Serge Candéias
Laboratoire de Chimie et Biologie des Métaux
François Chevalier
francois.chevalier@ganil.fr

Centre de Recherche sur les Ions, les Matériaux et la Photonique

---

Research Article

Keywords: Non-small cell lung cancer, KRAS inhibitor; Carbon ions irradiation, cancer stem cell

Posted Date: April 30th, 2026

DOI: https://doi.org/10.21203/rs.3.rs-9469593/v1

License: This work is licensed under a Creative Commons Attribution 4.0 International License.
Read Full License

Additional Declarations: No competing interests reported.

Version of Record: A version of this preprint was published at Molecular and Cellular Biochemistry on July 31st, 2026. See the published version at https://doi.org/10.1007/s11010-026-05668-x.

Abstract

Non-small cell lung cancer (NSCLC) with *KRAS*^{G12C} mutation is associated with poor prognosis and resistance to standard therapies. Sotorasib, a *KRAS*^{G12C} tyrosine kinase inhibitor, has shown clinical efficacy, yet its interaction with different irradiation modalities remains unclear. This study aimed to evaluate the potential radiosensitizing effect of Sotorasib in such mutated cells exposed to X-rays or carbon-ion (C-ions) irradiation.

Two human NSCLC cell lines (H358, *KRAS*^{G12C}; and A549, *KRAS*^{G12S}) were treated with Sotorasib alone or in combination with X-rays or C-ions irradiation (1–8 Gy). Cell viability, clonogenic survival, and sphere-forming ability were assessed. Cytokines secretion and mRNA expression of cancer stem cells and epithelial-mesenchymal transition (EMT) -associated markers were analyzed 24 h post-treatments.

Sotorasib alone specifically reduced the clonogenic capacity of H358 cells to ~ 30% while no effect was observed with A549 cells. Interestingly, Sotorasib combined with X-ray irradiation decreased clonogenic survival compared with either treatment alone, without evidence of synergy. In contrast, a synergistic effect was observed with C-ions in H358 cells ($\beta = -0.36$, 95% CI [− 0.52 to − 0.20], $p < 0.001$; enhancement ratio = 4.21 at SF2). C-ions irradiation alone markedly reduced sphere formation in both cell lines, whereas sotorasib showed no additional impact. GM-CSF expression was downregulated with sotorasib alone while IP-10 was upregulated when H358 cells were irradiated with sotorasib, suggesting an immune-specific modulatory response.

A specific radiosensitization of *KRAS*^{G12C} –mutated NSCLC cells was observed when associating Sotorasib with C-ions. This represents the first evidence of enhanced cytotoxicity from combining *KRAS*^{G12C} inhibition with high-LET radiation. These findings support further *in vivo* and translational studies exploring C-ions therapy as a promising strategy for *KRAS*^{G12C}–mutated NSCLC.

1 Introduction

Non-small cell lung cancer (NSCLC) is the most common lung cancer (80% of lung cancers). Locally advanced stage III NSCLC represent approximately 30% of NSCLC with a significant number of inoperable cancers. The prognosis of these locally advanced inoperable cancers remains poor with a 5-year survival of less than 50% [1].

The *KRAS* (Kirsten rat sarcoma viral oncogene homologue) proto-oncogene encodes a small GTPase protein that transmits growth and differentiation signals from the cell surface to the nucleus by cycling between an active GTP-bound state and an inactive GDP-bound state. Mutated forms of KRAS remains permanently active by staying bound to GTP and continuously send signals that promote uncontrolled cell growth. KRAS mutated inoperable stage III NSLC have been reported to be more resistant to chemoradiotherapy than non KRAS mutated [2]. Furthermore, data obtained from resected NSCLC found that *KRAS*^{G12C} mutation was associated with worst survival [3]. Recently, tyrosine kinase inhibitors (TKI)

targeting the $KRAS^{G12C}$ mutation have been reported to promote good responses in metastatic $KRAS^{G12C}$ mutated NSCLC [4–6]. G12C is a single point mutation with a Glycine-to-Cysteine substitution at codon 12 of the exon 2. This substitution favors the activated state of KRAS, resulting in a predominantly GTP-bound KRAS oncoprotein, amplifying signaling pathways that lead to oncogenesis. AMG-510, also called Sotorasib, is a $KRAS^{G12C}$ TKI that inhibits specifically and irreversibly $KRAS^{G12C}$ mutation by trapping the mutated protein in the inactive GDP-bound state [7]. Treatment with Sotorasib resulted in a response rate of approximately 40% in patients with $KRAS^{G12C}$ mutated NSCLC in a phase II clinical trial [5]. $KRAS^{G12C}$ inhibitors in association with chemoradiotherapy may represent a good strategy to improve response and survival in $KRAS^{G12C}$ mutated inoperable stage III NSCLC patients, indeed, *KRAS* mutated A549 cells were radiosentized by inhibiting mutated $KRAS^{G12S}$ expression with siRNA [8].

KRAS mutations contribute also to the establishment of an immunosuppressive tumor microenvironment by limiting effective T-cell infiltration and promoting the recruitment of suppressive immune populations [9]. Combining X-rays irradiation and KRAS pathways inhibitors such as MEK inhibitors [10] or KRAS inhibitors like Adagrasib [11] can reverse this immune suppressive effect of KRAS mutations and promote a pro inflammatory, anti-tumor phenotype.

Another radioresistance mechanism of tumors may be the presence of cancer stem cells (CSCs). CSCs are a subpopulation of dedifferentiated cancer cells with self-renewal capabilities and increased resistance to DNA damage, apoptosis, and oxidative stress [12]. CSCs are identified by specific stemness markers overexpressed in lung cancer such as CD166 [13] in adenocarcinoma lung cells. X-rays irradiation can up-regulate CSCs markers in lung cancer cells [14–16] leading to radioresistant phenotype selection. CSCs are mainly in hypoxic niches that could also explain this radioresistance effect [17, 18]. Cancer cells can acquire stem-like properties through epithelial–mesenchymal transition (EMT) [19]. EMT confers mesenchymal characteristics to epithelial cancer cells, including loss of polarity, downregulation of epithelial markers such as E-cadherin, upregulation of Nestin [20] and Vimetin [21], acquisition of enhanced migratory and invasive capacities [22]. EMT facilitates metastasis and tumor recurrence by enabling mesenchymal CSCs to disseminate to distant sites, where they can revert to an epithelial phenotype and initiate metastatic growth [23]. Vimentin, a key mesenchymal marker, is frequently upregulated in NSCLC, particularly in response to X-ray irradiation [14, 24]. Nestin is also upregulated in NSCLC [20, 25] and has been implicated in the regulation of redox homeostasis [26], a poorer tumor differentiation and an increased cancer cell proliferation [13].

Carbon-ions (C-ions) radiotherapy represents a promising modality in the management of radioresistant tumors due to its unique physical and biological properties. Owing to their high linear energy transfer (LET), C-ions deposit dense ionizations in the tissue at the end of the ion range (Bragg peak). This dense ionization produces clustered and complex DNA lesions that are difficult to repair, enhancing cell-killing efficacy compared with sparsely ionizing photons. The resulting increase in relative biological effectiveness (RBE), generally ranges from 1.5 to 3 for CSC depending on tissue type, dose, and LET

distribution [27, 28]. In conventional X-rays irradiation, indirect DNA damage through reactive oxygen species generated by water radiolysis is predominant, whereas high-LET radiation primarily induces direct DNA damage. Unlike X-ray irradiation, the cytotoxicity of C-ions is largely preserved under hypoxia due to their reduced dependence on oxygen conditions [29]. C-ions irradiation have been reported to be more effective on lung cancer cells in hypoxic niches [30, 31] and might be more effective on CSC. The combination of high RBE, low oxygen enhancement ratio, and the induction of complex, irreparable DNA damage provides a strong rationale for the use of C-ions radiotherapy in hypoxic niches enriched with CSCs, such as in NSCLC [32]. Japanese clinical series have demonstrated excellent local control (80–93% at 2 years) and favorable toxicity profiles for use of C-ions radiotherapy in NSCLC [33, 34].

To investigate how treatment efficiency could be increased by the combination of irradiation and $KRAS^{G12C}$ inhibitor in lung cancers, we conducted an *in vitro* study to determine the efficacy of combining the *KRAS* inhibitor Sotorasib in association with different qualities of irradiation (X-rays and C-ions irradiations) in a $KRAS^{G12C}$ mutated lung cancer cell line, target of Sotorasib and in a $KRAS^{G12S}$ mutated lung cancer cell line, used as a control cells. A specific and robust effect was observed when combining Sotorasib and high LET radiation, reducing the clonogenic survival and proliferation of $KRAS^{G12C}$ mutated cells, and inducing an antitumoral immune response.

2 Material and Methods

2.1 Cell culture

The human lung adenocarcinoma cell line A549 (Ref CCL-185) and the human bronchioalveolar carcinoma cell line H358 (Ref NCI-H358), were purchased from ATCC (Manassas, VA, USA). A549 cell line harboring *KRAS G12S* mutation was isolated from the lung tissue of a 58-year-old male with lung cancer. H358 cell line harboring *KRAS G12C* heterozygous mutation and *P53* homozygous deletion was isolated from the bronchiole of a male patient with bronchioalveolar carcinoma. All cell lines were cultured in RPMI medium (Merck KGaA, Darmstadt, Germany) supplemented with 10% fetal calf serum (Merck KGaA, Darmstadt, Germany), 2 mM glutamine (Merck KGaA, Darmstadt, Germany), and 1% antibiotics (penicillin-streptomycin, Merck KGaA, Darmstadt, Germany), at 37°C in a humidified atmosphere with 5% CO_2.

2.2 KRAS G12C inhibitors

Sotorasib (AMG-510) was purchased from MedChemExpress (New Jersey, USA) and used *in vitro* at 10 nM according to a dose response experiment. Sotorasib in DMSO at 10 mM was diluted to its final concentration with culture medium, and finally added to the cells 24 h before irradiation and left in the cell culture medium for 24 h. Negative control samples were treated with the same DMSO dilutions.

2.3 Irradiations

X-rays irradiation was performed using a Pxi XradSmart 225cX irradiator with a tube tension of 225 kV and an intensity of 10 mA, corresponding to a dose rate of 2 Gy/min. For gene expression and cytokine secretion analysis, H358 cells were exposed to X-rays in a Xstrahl-CIX2 cabinet (Xstrahl, United Kingdom), with an energy of 195 kV and a current of 12.5 mA.

C-ions irradiations were performed at GANIL (Caen, France), using the IRABAT beam line, with a native ^{12}C beam of 95 MeV/A in the plateau region before the Bragg peak. A 16.9-mm-thick PMMA was inserted between the exit of the beam and sample holder in order to reach a LET of 73 keV/µm (2 Gy = 1.71×10^7 particles/cm^2), as previously described [35].

2.4 Western blot

Following the irradiation and treatment (48 h after irradiation), the cells were washed with PBS, and the cell pellet was lysed in RIPA lysis buffer (Thermo Fisher Scientific, Waltham, MA USA), supplemented with 1X protease inhibitor cocktail (Thermo Fisher Scientific, Waltham, MA USA), as previously described [36]. The protein samples were then analyzed by western-blotting (see detailed protocol in **Sup data 1**) using tubuline, ERK and phospho-ERK antibodies.

2.5 Clonogenic assay

A549 and H358 cells were irradiated in T25 cm^2 flasks at cell confluency. A sham control was included to evaluate the plating efficiency. At 18–24 h after irradiation, the cells were harvested and re-plated at low density. Medium including Sotorasib or DMSO was changed every 2 to 3 days. Colonies were stained with crystal violet solution (0.3% w/v crystal violet in 20% v/v ethanol). Only colonies that comprised over 50 cells were counted by eye under a stereomicroscope. Clonogenic survival of H358 and A549 cells after irradiation was expressed as a function of dose and was normalized with non-irradiated samples. Surviving fractions of X-rays-irradiated samples were plotted using a linear quadratic and a linear model was used for those after C-ions irradiated samples. Delayed plating was used to avoid confounding effects of Sotorasib on colony formation. Immediate plating under continued drug-induced cell-cycle arrest could artificially reduce clonogenic growth independently of radiation-induced reproductive death. Allowing a recovery period before plating ensures that colony formation reflects true clonogenic survival following the combined treatment.

2.6 Proliferation assay

Cell proliferation was evaluated with the CellTrace® Far Red Cell Proliferation Kit (ThermoFisher Scientific, Waltham, MA USA) as previously described [37]. Experiments with X-rays and C-ions were analyzed with a Gallios flow cytometer (Beckman Coulter, Villepinte, France) at the ISOCELL platform (US PLATON, Caen, France). The data were acquired using Gallios software (Beckman Coulter). Data were analyzed with FCS Express 6+ (DeNovo®), and proliferation index were calculated by the software using the non-divided control as reference. Control and irradiated samples were compared with the corresponding Sotorasib-treated samples at the same irradiation dose to evaluate the radiosensitizing effect, defined as the enhancement factor.

2.7 Tumorspheres assay

A549 and H358 cells were plated 24 hours after irradiation at 5,000 cells/mL in 96 wells treated to prevent cell adhesion (Corning Costar Ultra-Low Attachment Multiple Well Plate). The culture medium was DMEM F12 (Sigma- Aldrich, D6421), supplemented with 0.5 µL/mL of βFGF and EGF, 10 µL/mL of PS, glutamine, and 3.6% hydrocortisone and finally 20µL/mL of insulin. The plates were supplemented every 2 or 3 days with DMEM medium at 5 µL/mL of EGF and βFGF. The number of spheres formed (from a cell that successfully proliferated without adhering) was counted after 10 days of culture (spheres with a diameter of more than 50 µm).

2.8 RTq PCR

Total RNA extraction from control and treated cells, cDNA synthesis and real time qPCR were performed as previously described [38]. Sequences of primers used to amplify human Nestin, Vimentin and CD166 transcripts are provided in **sup table 1**.

2.9 Cytokines quantification

The quantification of secreted cytokine in the supernatant of control and treated H358 cells was performed as previously described [39].

2.10 Statistics

The statistical analysis for cell proliferation, CSC markers, cytokines, and tumorsphere assays was performed using the statistical software Graph Prism with different statistic tests depending on normal distribution (two-way Anova test, Mann-Whitney U + FDR). Data were considered to be significantly different when $p < 0.05$.

Cell survival fractions data were analyzed using linear mixed models. Cell counts were first normalized to the initial number of seeded cells. For each experimental condition, the surviving fraction was calculated by normalizing to the corresponding 0 Gy control within each experiment. The surviving fraction was log-transformed prior to analysis.

The models included treatment, radiation type, and their interaction term as fixed effect, with experiment included as a random intercept to account for between-experiment variability. The interaction term was used to assess departure from additivity between treatment and irradiation. Estimated coefficients are reported with their 95% confidence intervals (95% CI). The surviving fraction at 2 Gy (SF2) was analyzed using a two-way ANOVA with treatment and radiation quality as fixed factors. Enhancement ratios (ER) were calculated at 2 Gy (SF2) by comparing survival fractions between treated and untreated conditions and are reported as descriptive measures of radiosensitization. The dose required to achieve 10% survival (D10) was derived from fitted survival curves.

3 Results

3.1 Sotorasib reduced clonogenic survival in H358 cells

In order to select an appropriate concentration of Sotorasib for all experiments, we tested the effects of different concentration of Sotorasib on ERK phosphorylation, a downstream signalization pathway of KRAS by western blot assays. We observed a specific reduction of phospho-ERK, in H358 cells at a concentration of 10 nM (**sup data 1**). Using this Sotorasib concentration, clonogenic survival in H358 cells was about 30% ($p < 0{,}001$) (Fig. 1A, **left**) with a characteristic reduction of clone size. As expected, Sotorasib had no effect on clonogenic behavior in A549 cells (Fig. 1A, **right)**.

3.2 Sotorasib enhances the radiosensitivity of H358 cells to carbon ions but not to X-rays

Sotorasib (10 nM) reduced the survival fraction of H358 cells with all irradiation doses compared to irradiated cells without drug **(**Fig. 1B, **left)**, whereas no effect was observed on A549 cells **(**Fig. 1B, **right)**.

In H358 cells, the surviving fraction at 2 Gy (SF2) was significantly reduced when Sotorasib was combined with C-ions irradiation compared with C-ions alone ($p < 0.005$), with a corresponding enhancement ratio (ER) of 4.21. Statistical analysis confirmed a synergistic interaction between Sotorasib and C-ions ($\beta = -0.36$, 95% CI [− 0.52; −0.20], $p < 0.001$).

In contrast, no evidence of a synergistic interaction was observed with X-ray irradiation ($\beta = 0.04$, 95% CI [− 0.02; 0.10], $p = 0.23$), and no significant reduction in SF2 was detected, with a corresponding ER of 1.02 (Table 1). Consistently, the dose required to achieve 10% survival (D10) was reduced by factors of 1.09 and 2.4 when Sotorasib was combined with X-rays and carbon ions, respectively.

Table 1
Calculated parameters of H358 and A549 cells survival after irradiation with X-rays and C-ions with and without Sotorasib

Conditions	H358				A589			
	SF2[a] (%)	D10[b] (Gy)	ER (SF2) [c]	ER (D10) [d]	SF2[a] (%)	D10[b] (Gy)	ER (SF2) [c]	ER (D10) [d]
X-rays	51	5,8	/	/	60	7,2		
X-rays + Sotorasib	50	5,3	1,02	1,09	88	7,1	0,68	1,01
C-ions	21,5	3,6	/	/	12,7	2,2		
C-ions + Sotorasib	5,1*	1,5	4,21	2,4	15,5	2,8	0,82	0,79
a: SF2: surviving fraction (%) at 2 Gy.								
b: D10: dose required to achieve 10% surviving fraction.								
c: ER (SF2): enhancement ratio calculated as SF2 (with Sotorasib) / SF2 (without Sotorasib).								
d: ER (D10): enhancement ratio calculated as D10 (with Sotorasib) / D10 (without Sotorasib).								
Statistical significance was assessed for SF2 values only. Enhancement ratios (ER) are descriptive and were not statistically tested. * $p < 0.05$ compared with corresponding irradiation condition without Sotorasib.								

3.3 Sotorasib decreased cell proliferation in combination with C-ions irradiation

Sotorasib alone reduced the proliferation index of H358 cells by approximately 35% ($p < 0.05$; Fig. 2), while no significant effect was observed in A549 cells. X-ray irradiation alone did not alter the cellular index in H358 cells; however, its combination with Sotorasib further decreased the index by 41–44% at 1, 2, and 4 Gy compared with irradiation alone ($p < 0.05$). Carbon-ion irradiation alone reduced the cellular index of H358 cells by 26.5%, 64%, and 83% at 1, 2, and 4 Gy, respectively ($p < 0.05$). When combined with Sotorasib, C-ion irradiation at 1 and 2 Gy produced greater decreases of 67% and 82%, ($p < 0.05$) with the corresponding enhancement factors of 1.55 at 1 Gy and 1.50 at 2 Gy ($p < 0.05$). In contrast, the reduced proliferation index observed in C-ions-irradiated A549 cells is not further modulated in the presence of Sotorasib.

3.4 Sotorasib did not impact tumor-spheres formation and CSC markers expression

Sphere formation was reduced by X-ray at 1 Gy in H358 and 2 Gy in A549 (Fig. 3 **top**). C-ions irradiations reduced the formation of spheres in both A549 and H358 cell lines (Fig. 3 **bottom**). The addition of

Sotorasib alone or with irradiations did not alter any sphere formation in H358 and A549 cells. This observation was confirmed with the quantification of selected CSC and EMT mRNA markers in H358 cells. Sotorasib alone, X-rays, C-ion and combinations did not affect CD166, Vimentin or Nestin expression in H358 cells (**sup data 2**).

3.5 Sotorasib induced pro-inflammatory and immune anti-tumor phenotype

Secretions of pro- and anti-inflammatory cytokines were measured in H358 cells after exposure to Sotorasib combined with irradiations **(**Fig. 4).

Sotorasib alone showed a trend toward increased IP-10 secretion, a pro-inflammatory cytokine, at 24 hours in H358 cells **(**Fig. 4, A) with a significant upregulation of IP-10 secretion 24 hours after X-ray irradiation at 2 and 4 Gy ($p < 0.05$), a similar upward trend at 8 Gy and across all doses of carbon-ion irradiation (2–8 Gy).

The secretion of GM-CSF, involved in the establishment of an immunosuppressive microenvironment, is reduced by Sotorasib alone **(**Fig. 4, B). C-ions irradiation at 8 Gy significantly upregulated GM-CSF secretion in H358 cells, 24 h post-irradiation ($p < 0.05$). This effect was reversed when combined with Sotorasib, which led to a significant downregulation of GM-CSF at 8 Gy ($p < 0.05$). A similar decreasing trend in GM-CSF secretion was observed at all C-ions doses. In contrast, Sotorasib did not affect GM-CSF secretion when combined with X-rays irradiation in H358 cells.

In contrast, Sotorasib—either alone or combined with X-rays or C-ions irradiation—did not modify IL-6 secretion 24 hours after irradiation **(**Fig. 4, C).

4 Discussion

In our study, Sotorasib in combination with X-ray irradiation reduced clonogenic survival compared with either treatment alone; however, no evidence of a radiosensitizing or synergistic interaction was observed in H358 cells.H358 cells harbor *KRAS* ^{G12C} heterozygote mutation. Consistently, Adagrasib, another KRAS^{G12C} inhibitor, has been shown to enhance sensitivity to X-ray in *KRAS*^{G12C} homozygous mutant cells (CT26, a murine colorectal carcinoma line) but not in heterozygous mutant cells (LL2, a murine Lewis lung carcinoma line), both in vitro and in mouse models [11].

In contrast, Sotorasib exhibited a synergistic radio-sensitizing effect in H358 cells when combined with C-ions irradiation. To our knowledge, this is the first report of such an effect in human *KRAS*^{G12C}–mutated cell lines. While C-ions irradiation alone reduced tumor sphere formation, neither Sotorasib nor X-ray irradiation produced a similar effect. Tumor spheres are cell aggregates that grow under non-adherent conditions, as a surrogate indicator of CSC [40] and radioresistance [16]. Sotorasib did not affect the formation of non-adherent spheres, suggesting the persistence of a subpopulation of cells

that is not responsive to KRAS G12C inhibition. This observation is consistent with previously reported intrinsic and acquired resistance mechanisms to Sotorasib in NSCLC [5], including adaptive pathway reactivation and cellular heterogeneity. Such resistant cells may exhibit stem-like properties and contribute to tumorsphere formation, which is commonly used as a surrogate for self-renewal capacity. In this context, the persistence of sphere-forming cells may reflect a reservoir of drug-tolerant or resistant cells that could underlie tumor relapse. The effect of high LET C-ions on tumor spheres suggests that C-ions may target a cancer cell population distinct from that affected by Sotorasib.

Nestin, an EMT marker, is overexpressed in NSCLC cells following X-ray irradiation and has been associated with increased resistance to oxidative stress [41]. Vimentin, another EMT marker, is commonly overexpressed in various lung cancers [24], while CD166 is frequently expressed in lung adenocarcinomas and is considered a potential CSC marker [13]. In our study, the expression of these EMT and CSC markers showed high variability (data not shown) and was not significantly changed after treatment with Sotorasib, X-rays, or C-ions irradiation. Further investigations are required to determine which CSC subpopulations might be specifically targeted by C-ions irradiation of H358 cells.

Sotorasib has been reported to promote a pro-inflammatory tumor microenvironment in mouse models [7] and $KRAS^{G12C}$ inhibitors such as Adagrasib, when combined with X-ray irradiation, have been shown to elicit anti-tumor immune responses in vivo [11]. In our study, Sotorasib induced an overexpression of IP-10 and decreased the expression of GM-CSF. GM-CSF can contribute to tumor progression [42] while IP-10 expression has been shown to sensitize tumors to immune checkpoint inhibitors by promoting $CD8^+$ T-cell recruitment [43]. Our findings suggest that Sotorasib combined with either X-ray or C-ion irradiation can affect cytokine secretion so that the immune microenvironment is modulated to promote the development of a pro-inflammatory, anti-tumor immune contexture.

Further investigations on CSCs, EMT markers, and cytokines are still needed in order to elucidate mechanisms underlying the efficacy of combining irradiation with Sotorasib in NSCLC.

5 Conclusion

In this study, we first demonstrated the specific radio-sensitizing effect of combining high LET C-ions irradiation with Sotorasib in a $KRAS^{G12C}$-mutated NSCLC cell line. This effect was observed despite the heterozygous, rather than homozygous, KRAS mutation in H358 cells. These findings support further investigation of the combination of C-ions and KRAS inhibitors in NSCLC, as they may target distinct cancer cell populations and thereby improve therapeutic responses. Additional in vitro and in vivo studies are warranted to elucidate the underlying mechanisms prior to clinical translation.

Declarations

6 Acknowledgements

The authors want to thank Clément Rouichi, from IRIG-LCBM laboratory and Marilyne Guillamin from the Isocell Cytometry Platform (Service Unit PLATON, University of Caen Normandie) for their technical support. Finally, the authors want to thank the GANIL and CIMAP-CIRIL facilities staff for C-ions calibration and dosimetry.

7 Funding

This work was supported by a Grant of “Ligue contre le Cancer – comité de Seine Maritime”, 2022-2023, « Traitement par inhibiteurs de KRAS en association avec l’irradiation X vs ions carbone dans le cancer bronchique non à petite cellule (CBNPC) avec mutation KRAS », by a Grant of Electricité de France 2023-2025, funding from committee « Protection de l’Homme et de l’Environnement (CPPHE) », under the Life Sciences group of the four-way national agreement CEA-EDF-IRSN-Framatome, “Rôle de KRAS dans la modulation de la radiorésistance et du statut inflammatoire dans le cancer bronchique non à petites cellules” by the LABEX PRIMES (grant number ANR-11-LABX-0063), and by GRAL, a program from the Chemistry Biology Health (CBH) Graduate School of University Grenoble Alpes (grant number ANR-17-EURE-0003). Irradiations with C-ions were performed at GANIL (Caen, France) using beam times obtained under experiment number P1317-H (KRAS Inhibitors treatment in association with X vs hadrons Radiations in non-small cell lung cancer” of the iPAC 2022 call, CIMAP-CIRIL.

8 Conflicts of interest

none

9 Ethics declaration:

not applicable

10 Authors’ contribution:

Mathieu Césaire: Formal analysis, Methodology, Writing – original draft, Writing – review and editing. Kilian Lecrosnier: Formal analysis, Methodology. Juliette Montanari: Formal analysis, Methodology. Mateusz Sitarz: Formal analysis, Methodology, Writing – original draft. Sahra Messaoudi: Methodology, Writing – original draft. Elisabeth Chartier-Garcia: Formal analysis, Methodology. Isabelle Testard: Formal analysis, Methodology, Writing – original draft. Guénaëlle Levallet: Writing – review and editing. Serge Candéias: Formal analysis, Methodology, Writing – original draft, Writing – review and editing. François Chevalier: Conceptualization, Formal analysis, Funding acquisition, Investigation, Methodology, Project administration, Supervision, Validation, Visualization, Writing – original draft, Writing – review and editing.

References

1. Antonia SJ, Villegas A, Daniel D, Vicente D, Murakami S, Hui R, Kurata T, Chiappori A, Lee KH, de Wit M, Cho BC, Bourhaba M, Quantin X, Tokito T, Mekhail T, Planchard D, Kim Y-C, Karapetis CS, Hiret S,

Ostoros G, Kubota K, Gray JE, Paz-Ares L, de Castro Carpeño J, Faivre-Finn C, Reck M, Vansteenkiste J, Spigel DR, Wadsworth C, Melillo G, Taboada M, Dennis PA, Özgüroğlu M, PACIFIC Investigators (2018) Overall Survival with Durvalumab after Chemoradiotherapy in Stage III NSCLC. N Engl J Med 379:2342–2350. https://doi.org/10.1056/NEJMoa1809697

2. Yagishita S, Horinouchi H, Sunami KS, Kanda S, Fujiwara Y, Nokihara H, Yamamoto N, Sumi M, Shiraishi K, Kohno T, Furuta K, Tsuta K, Tamura T, Ohe Y (2015) Impact of KRAS mutation on response and outcome of patients with stage III non-squamous non-small cell lung cancer. Cancer Sci 106:1402–1407. https://doi.org/10.1111/cas.12740
3. Finn SP, Addeo A, Dafni U, Thunnissen E, Bubendorf L, Madsen LB, Biernat W, Verbeken E, Hernandez-Losa J, Marchetti A, Cheney R, Warth A, Speel E-JM, Quinn AM, Monkhorst K, Jantus-Lewintre E, Tischler V, Marti N, Dimopoulou G, Molina-Vila MA, Kammler R, Kerr KM, Peters S, Stahel RA, European Thoracic Oncology Platform Lungscape Investigators (2021) Prognostic Impact of KRAS G12C Mutation in Patients With NSCLC: Results From the European Thoracic Oncology Platform Lungscape Project. J Thorac Oncol Off Publ Int Assoc Study Lung Cancer 16:990–1002. https://doi.org/10.1016/j.jtho.2021.02.016
4. Hong DS, Fakih MG, Strickler JH, Desai J, Durm GA, Shapiro GI, Falchook GS, Price TJ, Sacher A, Denlinger CS, Bang Y-J, Dy GK, Krauss JC, Kuboki Y, Kuo JC, Coveler AL, Park K, Kim TW, Barlesi F, Munster PN, Ramalingam SS, Burns TF, Meric-Bernstam F, Henary H, Ngang J, Ngarmchamnanrith G, Kim J, Houk BE, Canon J, Lipford JR, Friberg G, Lito P, Govindan R, Li BT (2020) KRASG12C Inhibition with Sotorasib in Advanced Solid Tumors. N Engl J Med 383:1207–1217. https://doi.org/10.1056/NEJMoa1917239
5. Koga T, Suda K, Fujino T, Ohara S, Hamada A, Nishino M, Chiba M, Shimoji M, Takemoto T, Arita T, Gmachl M, Hofmann MH, Soh J, Mitsudomi T (2021) KRAS Secondary Mutations That Confer Acquired Resistance to KRAS G12C Inhibitors, Sotorasib and Adagrasib, and Overcoming Strategies: Insights From In Vitro Experiments. J Thorac Oncol Off Publ Int Assoc Study Lung Cancer 16:1321–1332. https://doi.org/10.1016/j.jtho.2021.04.015
6. (2022) Adagrasib Response Remains Strong in NSCLC. Cancer Discov 12:OF1. https://doi.org/10.1158/2159-8290.CD-NB2022-0042
7. Canon J, Rex K, Saiki AY, Mohr C, Cooke K, Bagal D, Gaida K, Holt T, Knutson CG, Koppada N, Lanman BA, Werner J, Rapaport AS, San Miguel T, Ortiz R, Osgood T, Sun J-R, Zhu X, McCarter JD, Volak LP, Houk BE, Fakih MG, O'Neil BH, Price TJ, Falchook GS, Desai J, Kuo J, Govindan R, Hong DS, Ouyang W, Henary H, Arvedson T, Cee VJ, Lipford JR (2019) The clinical KRAS(G12C) inhibitor AMG 510 drives anti-tumour immunity. Nature 575:217–223. https://doi.org/10.1038/s41586-019-1694-1
8. Choi EJ, Ryu YK, Kim SY, Wu HG, Kim JS, Kim IH, Kim IA (2010) Targeting epidermal growth factor receptor-associated signaling pathways in non-small cell lung cancer cells: implication in radiation response. Mol Cancer Res MCR 8:1027–1036. https://doi.org/10.1158/1541-7786.MCR-09-0507
9. Xu M, Zhao X, Wen T, Qu X (2024) Unveiling the role of KRAS in tumor immune microenvironment. Biomed Pharmacother Biomedecine Pharmacother 171:116058. https://doi.org/10.1016/j.biopha.2023.116058

10. Zheng Y, Liu Y, Zhang F, Su C, Chen X, Zhang M, Sun M, Sun Y, Xing L (2022) Radiation combined with KRAS-MEK inhibitors enhances anticancer immunity in KRAS-mutated tumor models. Transl Res J Lab Clin Med S1931–5244(22):00178–00175. https://doi.org/10.1016/j.trsl.2022.08.005
11. Laurent P-A, Milic M, Quevrin C, Meziani L, Liu W, Morel D, Signolle N, Clémenson C, Levy A, Mondini M, Deutsch E (2023) KRASG12C inhibition using MRTX1257: a novel radio-sensitizing partner. J Transl Med 21:773. https://doi.org/10.1186/s12967-023-04619-0
12. Soundararajan L, Warrier S, Dharmarajan A, Bhaskaran N (2024) Predominant factors influencing reactive oxygen species in cancer stem cells. J Cell Biochem 125:3–21. https://doi.org/10.1002/jcb.30506
13. Sterlacci W, Savic S, Fiegl M, Obermann E, Tzankov A (2014) Putative stem cell markers in non-small-cell lung cancer: a clinicopathologic characterization. J Thorac Oncol Off Publ Int Assoc Study Lung Cancer 9:41–49. https://doi.org/10.1097/JTO.0000000000000021
14. Gomez-Casal R, Bhattacharya C, Ganesh N, Bailey L, Basse P, Gibson M, Epperly M, Levina V (2013) Non-small cell lung cancer cells survived ionizing radiation treatment display cancer stem cell and epithelial-mesenchymal transition phenotypes. Mol Cancer 12:94. https://doi.org/10.1186/1476-4598-12-94
15. Raei M, Bagheri M, Aghaabdollahian S, Ghorbani M, Sadeghi A (2022) Ionizing Radiation Promotes Epithelial-Mesenchymal Transition Phenotype and Stem Cell Marker in The Lung adenocarcinoma: In Vitro and Bioinformatic Studiesc. Cell J 24:522–530. https://doi.org/10.22074/cellj.2022.8403
16. Tsolou A, Lamprou I, Fortosi A-O, Liousia M, Giatromanolaki A, Koukourakis MI (2019) Stemness and senescence related escape pathways are dose dependent in lung cancer cells surviving post irradiation. Life Sci 232:116562. https://doi.org/10.1016/j.lfs.2019.116562
17. Iida H, Suzuki M, Goitsuka R, Ueno H (2012) Hypoxia induces CD133 expression in human lung cancer cells by up-regulation of OCT3/4 and SOX2. Int J Oncol 40:71–79. https://doi.org/10.3892/ijo.2011.1207
18. Das B, Tsuchida R, Malkin D, Koren G, Baruchel S, Yeger H (2008) Hypoxia enhances tumor stemness by increasing the invasive and tumorigenic side population fraction. Stem Cells Dayt Ohio 26:1818–1830. https://doi.org/10.1634/stemcells.2007-0724
19. Doherty MR, Smigiel JM, Junk DJ, Jackson MW (2016) Cancer Stem Cell Plasticity Drives Therapeutic Resistance. Cancers 8:8. https://doi.org/10.3390/cancers8010008
20. Bernal A, Arranz L (2018) Nestin-expressing progenitor cells: function, identity and therapeutic implications. Cell Mol Life Sci CMLS 75:2177–2195. https://doi.org/10.1007/s00018-018-2794-z
21. Satelli A, Li S (2011) Vimentin in cancer and its potential as a molecular target for cancer therapy. Cell Mol Life Sci CMLS 68:3033–3046. https://doi.org/10.1007/s00018-011-0735-1
22. Chung B-M, Rotty JD, Coulombe PA (2013) Networking galore: Intermediate filaments and cell migration. Curr Opin Cell Biol 25:600–612. https://doi.org/10.1016/j.ceb.2013.06.008
23. Chang JC (2016) Cancer stem cells: Role in tumor growth, recurrence, metastasis, and treatment resistance. Med (Baltim) 95:S20–S25. https://doi.org/10.1097/MD.0000000000004766

24. Bhardwaj M, Sen S, Chosdol K, Bakhshi S, Pushker N, Sharma A, Kashyap S, Bajaj MS, Singh VK (2020) Vimentin overexpression as a novel poor prognostic biomarker in eyelid sebaceous gland carcinoma. Br J Ophthalmol 104:879–884. https://doi.org/10.1136/bjophthalmol-2018-313285
25. Takakuwa O, Maeno K, Kunii E, Ozasa H, Hijikata H, Uemura T, Kasai D, Ohkubo H, Miyazaki M, Oguri T, Niimi A (2013) Involvement of intermediate filament nestin in cell growth of small-cell lung cancer. Lung Cancer Amst Neth 81:174–179. https://doi.org/10.1016/j.lungcan.2013.04.022
26. Wang J, Lu Q, Cai J, Wang Y, Lai X, Qiu Y, Huang Y, Ke Q, Zhang Y, Guan Y, Wu H, Wang Y, Liu X, Shi Y, Zhang K, Wang M, Peng Xiang A (2019) Nestin regulates cellular redox homeostasis in lung cancer through the Keap1-Nrf2 feedback loop. Nat Commun 10:5043. https://doi.org/10.1038/s41467-019-12925-9
27. Sai S, Wakai T, Vares G, Yamada S, Kamijo T, Kamada T, Shirai T (2015) Combination of carbon ion beam and gemcitabine causes irreparable DNA damage and death of radioresistant pancreatic cancer stem-like cells in vitro and in vivo. Oncotarget 6:5517–5535. https://doi.org/10.18632/oncotarget.3584
28. Cui X, Oonishi K, Tsujii H, Yasuda T, Matsumoto Y, Furusawa Y, Akashi M, Kamada T, Okayasu R (2011) Effects of carbon ion beam on putative colon cancer stem cells and its comparison with X-rays. Cancer Res 71:3676–3687. https://doi.org/10.1158/0008-5472.CAN-10-2926
29. Subtil FSB, Wilhelm J, Bill V, Westholt N, Rudolph S, Fischer J, Scheel S, Seay U, Fournier C, Taucher-Scholz G, Scholz M, Seeger W, Engenhart-Cabillic R, Rose F, Dahm-Daphi J, Hänze J (2014) Carbon ion radiotherapy of human lung cancer attenuates HIF-1 signaling and acts with considerably enhanced therapeutic efficiency. FASEB J Off Publ Fed Am Soc Exp Biol 28:1412–1421. https://doi.org/10.1096/fj.13-242230
30. Klein C, Dokic I, Mairani A, Mein S, Brons S, Häring P, Haberer T, Jäkel O, Zimmermann A, Zenke F, Blaukat A, Debus J, Abdollahi A (2017) Overcoming hypoxia-induced tumor radioresistance in non-small cell lung cancer by targeting DNA-dependent protein kinase in combination with carbon ion irradiation. Radiat Oncol Lond Engl 12:208. https://doi.org/10.1186/s13014-017-0939-0
31. Subtil FSB, Wilhelm J, Bill V, Westholt N, Rudolph S, Fischer J, Scheel S, Seay U, Fournier C, Taucher-Scholz G, Scholz M, Seeger W, Engenhart-Cabillic R, Rose F, Dahm-Daphi J, Hänze J (2014) Carbon ion radiotherapy of human lung cancer attenuates HIF-1 signaling and acts with considerably enhanced therapeutic efficiency. FASEB J Off Publ Fed Am Soc Exp Biol 28:1412–1421. https://doi.org/10.1096/fj.13-242230
32. Ancel J, Perotin J-M, Dewolf M, Launois C, Mulette P, Nawrocki-Raby B, Dalstein V, Gilles C, Deslée G, Polette M, Dormoy V (2021) Hypoxia in Lung Cancer Management: A Translational Approach. Cancers 13:3421. https://doi.org/10.3390/cancers13143421
33. Hayashi K, Yamamoto N, Nakajima M, Nomoto A, Tsuji H, Ogawa K, Kamada T (2019) Clinical outcomes of carbon-ion radiotherapy for locally advanced non-small-cell lung cancer. Cancer Sci 110:734–741. https://doi.org/10.1111/cas.13890

34. Takahashi W, Nakajima M, Yamamoto N, Yamashita H, Nakagawa K, Miyamoto T, Tsuji H, Kamada T, Fujisawa T (2015) A prospective nonrandomized phase I/II study of carbon ion radiotherapy in a favorable subset of locally advanced non-small cell lung cancer (NSCLC). Cancer 121:1321–1327. https://doi.org/10.1002/cncr.29195
35. Durantel F, Balanzat E, Cassimi A, Chevalier F, Ngono-Ravache Y, Madi T, Poully J-C, Ramillon J-M, Rothard H, Ropars F, Schwob L, Testard I, Saintigny Y (2016) Dosimetry for radiobiology experiments at GANIL. Nucl Instrum Methods Phys Res Sect Accel Spectrometers Detect Assoc Equip 816:70–77. https://doi.org/10.1016/j.nima.2016.01.052
36. Gilbert A, Tudor M, Delaunay A, Leman R, Levilly J, Atkinson A, Castéra L, Dinischiotu A, Savu DI, Valable S, Chevalier F (2024) Radiosensitizing Effect of PARP Inhibition on Chondrosarcoma and Chondrocyte Cells Is Dependent on Radiation LET. Biomolecules 14:1071. https://doi.org/10.3390/biom14091071
37. Césaire M, Ghosh U, Austry J-B, Muller E, Cammarata FP, Guillamin M, Caruso M, Castéra L, Petringa G, Cirrone GAP, Chevalier F (2019) Sensitization of chondrosarcoma cells with PARP inhibitor and high-LET radiation. J Bone Oncol 17:100246. https://doi.org/10.1016/j.jbo.2019.100246
38. Testard I, Garcia-Chartier E, Issa A, Collin-Faure V, Aude-Garcia C, Candéias SM (2023) Bystander signals from low- and high-dose irradiated human primary fibroblasts and keratinocytes modulate the inflammatory response of peripheral blood mononuclear cells. J Radiat Res (Tokyo) 64:304–316. https://doi.org/10.1093/jrr/rrac094
39. Gilbert A, Payet V, Bernay B, Chartier-Garcia E, Testard I, Candéias SM, Chevalier F (2022) Label-Free Direct Mass Spectrometry Analysis of the Bystander Effects Induced in Chondrocytes by Chondrosarcoma Cells Irradiated with X-rays and Carbon Ions. Front Biosci-Landmark 27:277. https://doi.org/10.31083/j.fbl2709277
40. Herreros-Pomares A, de-Maya-Girones JD, Calabuig-Fariñas S, Lucas R, Martínez A, Pardo-Sánchez JM, Alonso S, Blasco A, Guijarro R, Martorell M, Escorihuela E, Chiara MD, Duréndez E, Gandía C, Forteza J, Sirera R, Jantus-Lewintre E, Farràs R, Camps C (2019) Lung tumorspheres reveal cancer stem cell-like properties and a score with prognostic impact in resected non-small-cell lung cancer. Cell Death Dis 10:660. https://doi.org/10.1038/s41419-019-1898-1
41. Wang J, Lu Q, Cai J, Wang Y, Lai X, Qiu Y, Huang Y, Ke Q, Zhang Y, Guan Y, Wu H, Wang Y, Liu X, Shi Y, Zhang K, Wang M, Peng Xiang A (2019) Nestin regulates cellular redox homeostasis in lung cancer through the Keap1-Nrf2 feedback loop. Nat Commun 10:5043. https://doi.org/10.1038/s41467-019-12925-9
42. Gutschalk CM, Yanamandra AK, Linde N, Meides A, Depner S, Mueller MM (2013) GM-CSF enhances tumor invasion by elevated MMP-2, -9, and – 26 expression. Cancer Med 2:117–129. https://doi.org/10.1002/cam4.20
43. Limagne E, Nuttin L, Thibaudin M, Jacquin E, Aucagne R, Bon M, Revy S, Barnestein R, Ballot E, Truntzer C, Derangère V, Fumet J-D, Latour C, Rébé C, Bellaye P-S, Kaderbhaï C-G, Spill A, Collin B, Callanan MB, Lagrange A, Favier L, Coudert B, Arnould L, Ladoire S, Routy B, Joubert P, Ghiringhelli F

(2022) MEK inhibition overcomes chemoimmunotherapy resistance by inducing CXCL10 in cancer cells. Cancer Cell 40:136–152e12. https://doi.org/10.1016/j.ccell.2021.12.009

Figures

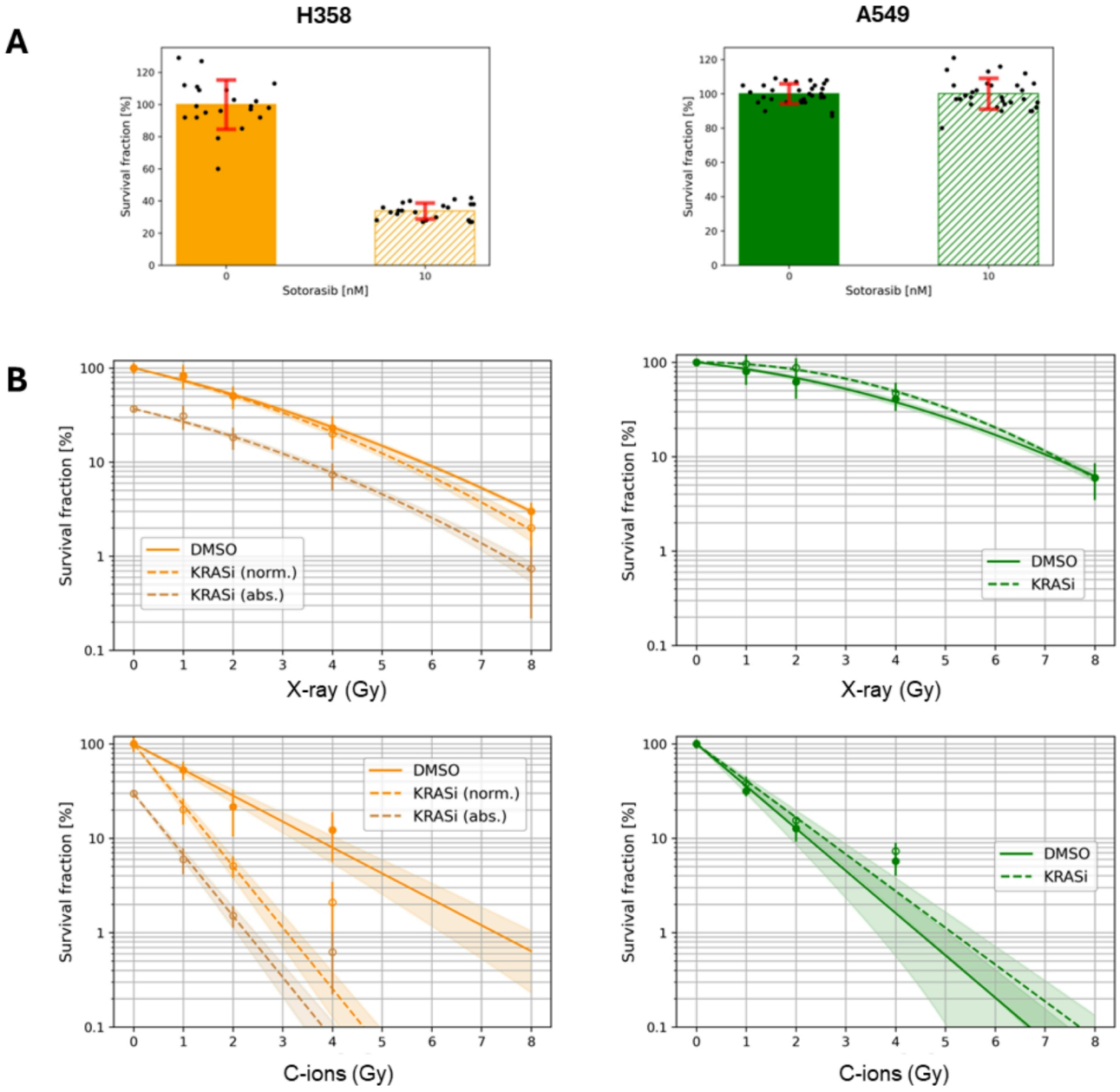

Figure 1

Sotorasib radiosensitized H358 cells in combination with Carbon ions irradiation but not with X-rays irradiation.

A: survival fraction of H358 cells (**left**) and A549 cells (**right**) after treatment with 10 nM sotorasib.

B: survival fraction (%) of H358 (**left in orange**) A549 (**right in green**) cells after irradiation with X-rays (**top**) or carbon ions (**bottom**) with 10 nM Sotorasib (**dotted line**) or without sotorasib (**solid line**). A red dotted line was added in case of H358, representing the effect of sotorasib without normalization on the non-irradiated control (100 %). Cell survival was represented as mean +/- SD of 3 independent experiments performed in triplicate for X-rays and C-ions. Survival curves were fitted according to the linear quadratic model (X-rays), or fitted and extrapolated according to a linear model (carbon ions).

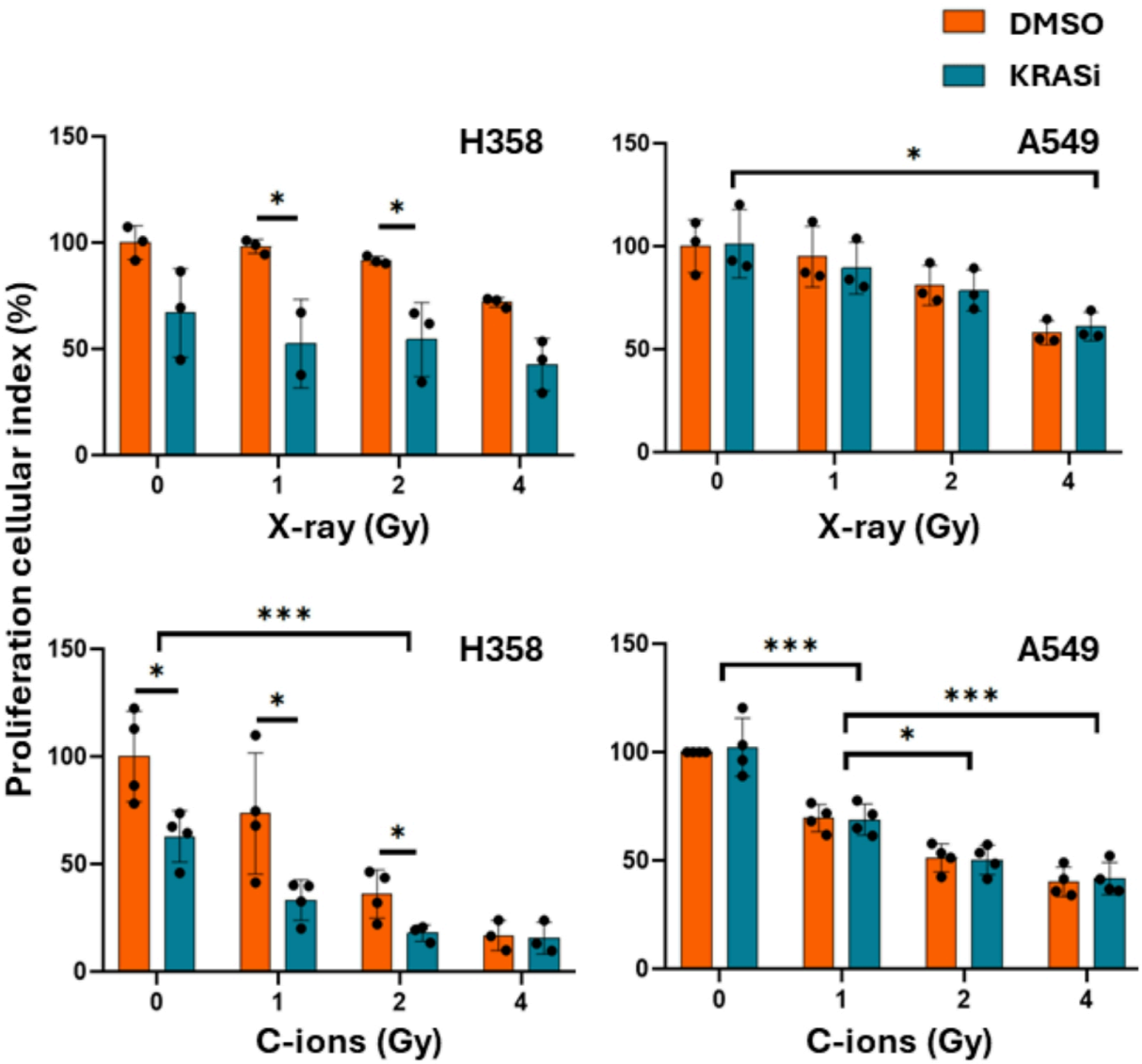

Figure 2

Sotorasib decreased cell proliferation in combination with Carbon ions irradiation.

Cell proliferation index of H358 cells (**left part**) and A549 cells (**right part**) following irradiation with X-rays (**top part**) or C-ions irradiation (**bottom part**) with DMSO as control (in orange) or KRASi (in blue). Proliferation indexes (%) are shown as mean +/- SD normalised on control without irradiation either KRASi with 3 independent experiments performed in triplicate. *p<0,05 et ***p<0,001 with a non-parametric two-way ANOVA test.

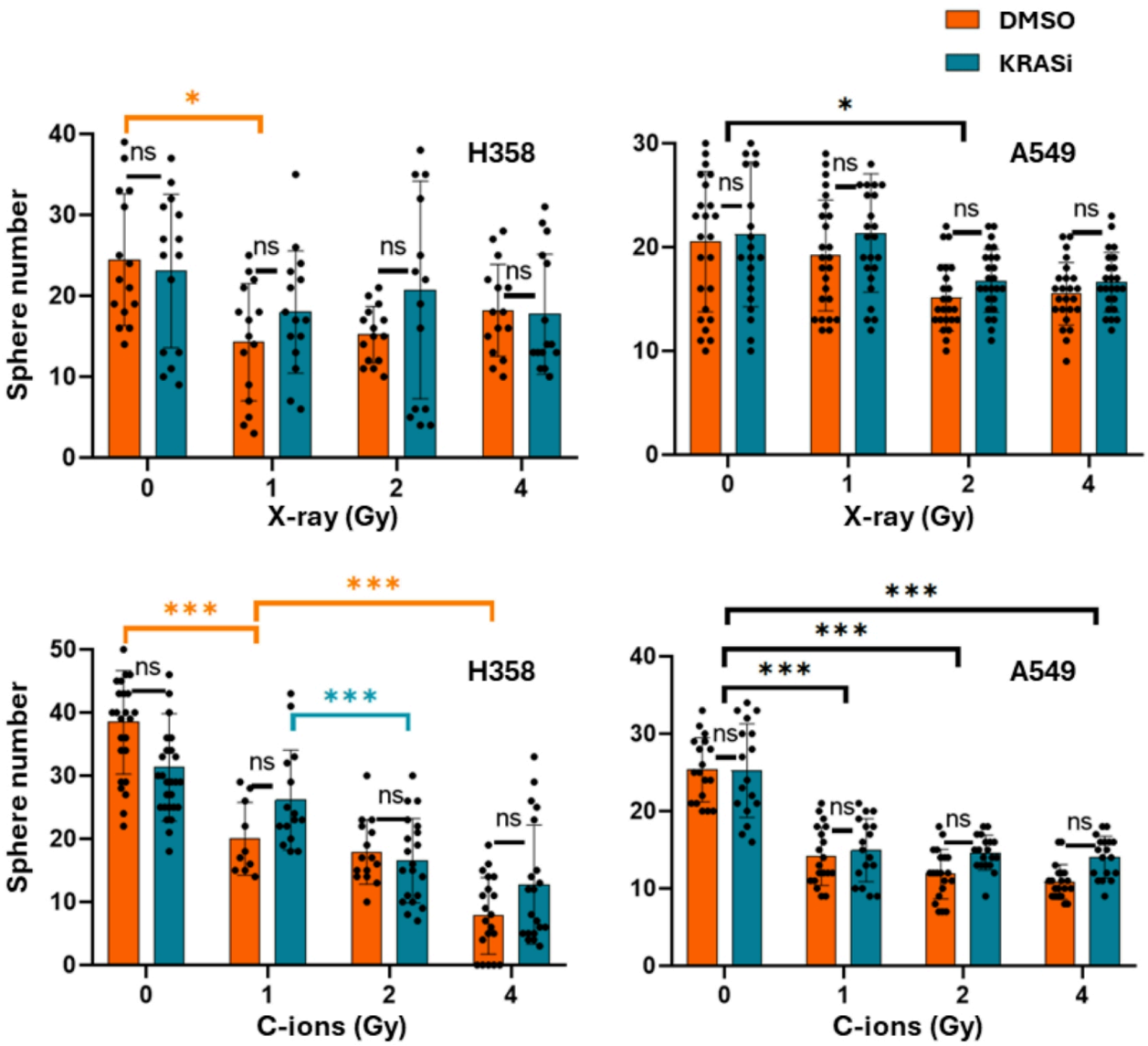

Figure 3

Growth of tumor spheres (> 50 µm) from H358 and A549 cells in non-adherent conditions.

Tumor sphere formation of H358 (**left part**) and A549 cells (**right part**) following treatment with X-rays (**top part**) or C-ions irradiation (**bottom part**) with DMSO as control (in orange) or KRASi (in blue). *p<0.05

and ***p<0.001 with a non-parametric two-way ANOVA test, ns = non-significant; black bar = dose-sample comparison; blue bar = KRASi-sample comparison; orange bar = DMSO-sample comparison.

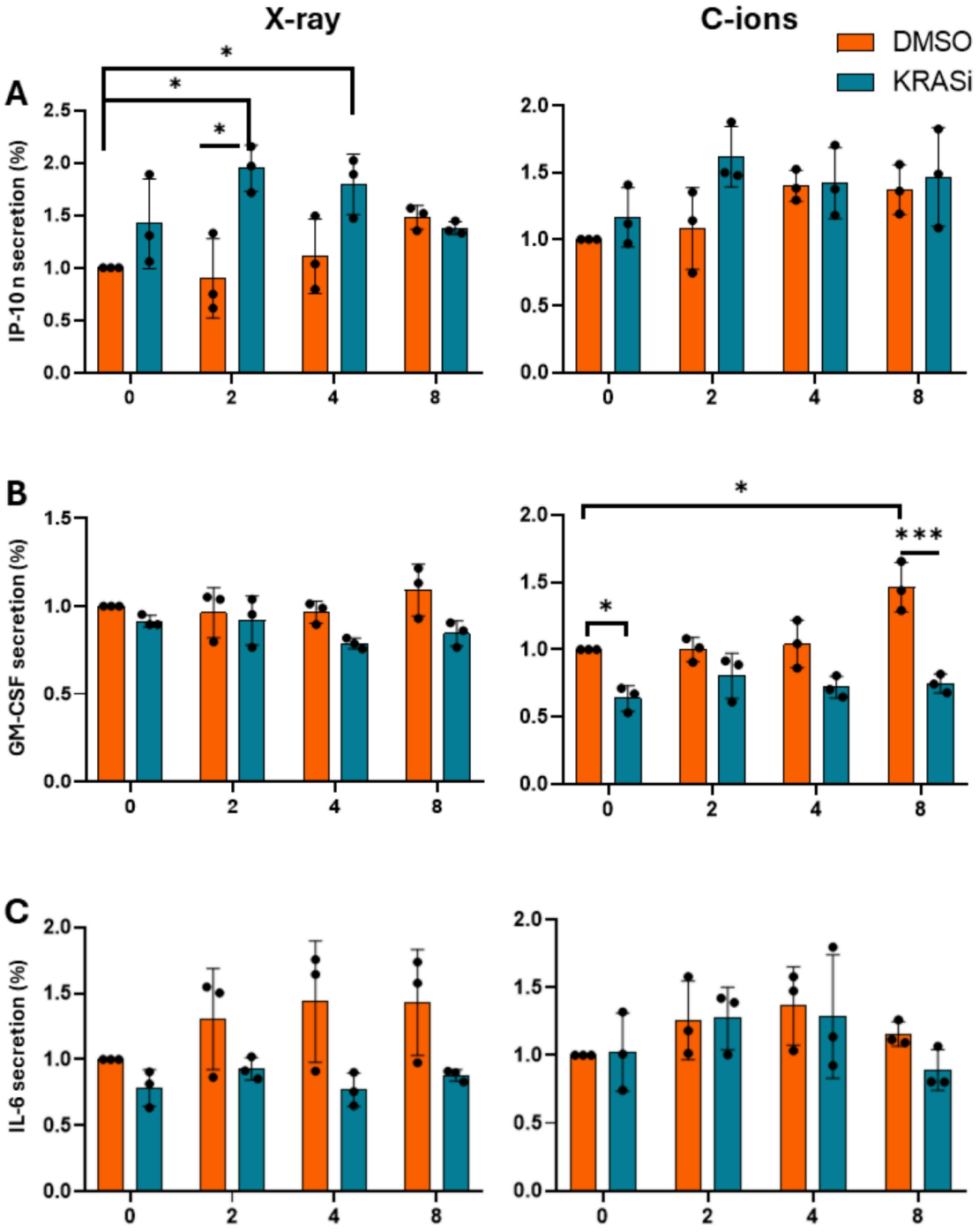

Figure 4

Relative expression of IP10, GM-CSF and IL-6 cytokines at 24h after treatment with Sotorasib and X-rays (left) or C-ions irradiation (right) in H358 cells.

Relative expressions of IP-10 (A), GM-CSF (B) and IL-6 (C) were expressed as a percentage of non-irradiated controls without Sotorasib. * $p<0.05$; ** $p<0.001$ with a non-parametric two-way ANOVA test.

Supplementary Files

This is a list of supplementary files associated with this preprint. Click to download.

- Supplementarymaterial.docx